CrossMark

ORIGINAL PAPER

Catalytic Conversion of Glucose to 5-Hydroxymethyfurfural Over B₂O₃ Supported Solid Acids Catalysts

Bin Han[1] · Peng Zhao[1] · Rong He[1] · Tinghua Wu[1] · Ying Wu[1]

Abstract A series of supported B_2O_3/ZrO_2–Al_2O_3 (BZA) catalysts with different loading B_2O_3 were prepared and characterized by XRD, FT-IR, XPS, NH_3-TPD, N_2 adsorption–desorption and FT-IR (pyridine adsorption). These catalysts were applied for direct conversion of glucose to 5-hydroxymethylfurfural (HMF). An optimized HMF yield of 41.2% at a glucose conversion of 90.8% was obtained within 4 h at 150 °C over B_2O_3 (20 wt%)/ZrO_2–Al_2O_3 (BZA-0.20). The best catalytic performance of BZA-0.20 was associated with the highest amount of total acid. The simultaneously bearing Lewis acid and Brønsted acid sites were more efficient for production of HMF from glucose.

Keywords Solid acid · Heterogeneous catalysts · 5-Hydroxymethylfurfural · Glucose

Introduction

The decreasing in nonrenewable fossil resources and the growing environmental awareness, have imposed the research for the sustainable resources as the alternatives.

✉ Tinghua Wu
  thwu@zjnu.cn

✉ Ying Wu
  yingwu@zjnu.cn

1   Key Laboratory of the Ministry of Education
    for Advanced Catalysis Materials, Institute of Physical
    Chemistry, Zhejiang Normal University, Jinhua 321004,
    People's Republic of China

Biomass as an abundant, renewable, ecofriendly and relative low cost novel energy sources [1–3], has been recognized as the most attractive substitute for production of chemicals. As one of most promising chemicals, the biomass-derived 5-hydroxymethylfurfural (HMF) plays a significant role in biobased energy, because it can be converted to various building blocks, which are widely applied to fine chemicals, pharmaceuticals, polymeric materials and the transportation liquid fuels [4–6].

The extensive research efforts have been focused on the novel methods of the conversion process from carbohydrates substrates to HMF. Conventionally, HMF is formed from hexoses (i.e., glucose and fructose) by eliminating triple moles of water [7]. Fructose has been shown to be easily dehydrated to HMF, although its drawback is that high cost and lower availability. In contrast, glucose is the preferred starting material since it is inexpensive, more abundant and readily available [8, 9]. However, the stable glucopyranose structure of glucose remains a challenge for synthesis of HMF. It is believed that HMF formation from glucose involves two consecutive steps: (1) glucose isomerization to fructose; (2) fructose dehydration to HMF. Lewis acid sites facilitate the first step, while Brønsted acid sites promote the later one [10, 11]. Therefore, searching for suitable catalytic systems is particularly essential for transformation of glucose to HMF.

In recent years, various catalytic system such as Lewis acidic metal halides [12], metal sulfates [13, 14], metal phosphates [15], polymeric material [16] and metal oxide [17] have been used for dehydration of glucose to HMF. Among the reported catalysts system, heterogeneous solid catalysts have attracted much attention over homogeneous, because they are environmentally benign, better recyclability, green chemical processes, ease of separation, and reduce corrosion to equipment [18].

Boric acid [B(OH)$_3$] has been identified as an active promoter for glucose-fructose isomerization [19, 20], and can also to be operational simplicity and non corrosiveness, thus make it as a promising alternative catalyst for production of HMF from glucose. In a study by Hansen and co-workers, B(OH)$_3$ was used to convert glucose into HMF in a biphasic system (H$_2$O/MIBK), a 14% yield of HMF at 41% glucose conversion can be obtained after 5 h at 150 °C [21]. Recently, Mayanka et al. reported that the yield of HMF from glucose can reach 81% using silica-supported boric acid and [bmim]HSO$_4$ catalytic system [22]. B$_2$O$_3$ has also been used in an earlier report for kinetic study of conversion of carbohydrates to HMF, which demonstrated that the complete conversion of the carbohydrate can be achieved in [BMIM]Cl [23]. Subsequently, Liu et al. reported that the yield of HMF from glucose can reach 41.4% using mesoporous B$_2$O$_3$–Al$_2$O$_3$ in DMSO solvent, and the catalyst was detected to have high specific surface area and strong Lewis acidic sites [24].

Several mental oxide, such as zirconia (ZrO$_2$) and alumina (Al$_2$O$_3$), have been as catalyst supports or solid acid catalysts employed in the reaction of dehydration of biomass to HMF. Moreover, structural property of these oxides could be significantly improved by mixing them together. This improvement is attributable to the generation of new catalytic sites due to strong interaction between the individual components, so that enhance the surface acid-base properties and thermal stability. Hence, we synthesized a series of supported bifunctional B$_2$O$_3$/ZrO$_2$–Al$_2$O$_3$ solid acid catalysts with Brønsted and Lewis acidic sites. For the first time, the catalyst was used for conversion of glucose to HMF in organic solvent to evaluate the catalytic performance. Meanwhile, the effects of various experimental parameters, such as B$_2$O$_3$ loading, reaction time and temperature, catalyst amount, reaction medium have also been explored in order to attain an optimized reaction conditions for production of HMF.

Experimental Section

Materials

D-Glucose (AR), 5-hydroxymethylfurfural (5-HMF, >99%), Zirconium (IV) oxychloride octahydrate (ZrOCl$_2$·8H$_2$O, AR), aluminum oxide (AR), ammonium hydroxide (28 wt%) were purchased from Sinopharm Chemical Reagent Co. Ltd. (Shanghai, China). boric acid (AR) was obtained from Shanghai Lianshi Chemical Co. Ltd. (Shanghai, China). dimethylsulfoxide (DMSO, AR), N,N-dimethylacetamide (DMAC, AR), N,N-dimethylformamide (DMF, AR) and N-methylpyrrolidone (NMP, AR) were supplied by Aladdin Chemistry Co. Ltd. (Shanghai,

China). All chemicals were used in this study without further purification.

Synthesis of B$_2$O$_3$/ZrO$_2$–Al$_2$O$_3$ Catalysts

Typically, B$_2$O$_3$/ZrO$_2$–Al$_2$O$_3$ catalyst was prepared by precipitation and impregnated method [25]. ZrOCl$_2$·8H$_2$O were dissolved in deionized water to prepare a solution after stirring 30 min, then the alumina powder was added to the solution under agitation(Zr/Al molar ratio = 5:5). Then ammonium hydroxide (28 wt%) was added dropwise to the solution to adjust the pH to 9–10 and precipitate the metal oxides. The formed precipitate in the solution was kept at room temperature for 24 h, filtered and washed with deionized water to remove chloride, and dried at 110 °C for 12 h. Then the precipitate was impregnated to the 50 ml boric acid solution with constant stirring to obtain slurry, then dried at 80 °C for 6 h. The prepared materials were calcined at 923 K for 5 h. The B$_2$O$_3$/ZrO$_2$–Al$_2$O$_3$ solid acid catalyst samples as ZA, BZA-0.05, BZA-0.10, BZA-0.15, BZA-0.20 and BZA-0.30 according to the B$_2$O$_3$ loading of 0, 5, 10, 15, 20 and 30%, respectively.

Catalyst Characterization

Powder XRD measurements were carried out using a Rigaku Dimax-3C with a monochromatic Cu Kα radiation (40 kV, 30 mA) in the 2θ range 10–80°. The transmission electron microscopy (TEM) were performed using a JEOLJEM-2100F instrument at an accelerating voltage of 200 kV. All FTIR spectra were recorded on a Nicolet NEXUS670 spectrometer (KBr discs) in the 4000−400 cm^{-1} region. The X-ray photoelectron spectrometer (XPS) were collected on a Escalab-250-Xi using a monochromatic Al Kα for the X-ray source. Binding energies were referenced to the C(1 s) binding energy of carbon, which was taken to be 284.8 eV. The specific surface areas of the catalysts were determined by N$_2$ adsorption–desorption measurements (CHEMET-3000), and the surface areas were calculated by the Brunauer–Emmett–Teller (BET) method. Temperature programmed desorption of ammonia (NH$_3$-TPD) were conducted on a Micromerictics Auto-Chem II 2920 instrument equipped with a TCD detector. About 100 mg sample was heated from room temperature to 100 °C with a heating rate of 10 $^{\circ}$C/min under He flow, and maintained at this temperature for 60 min. The sample was cooled to room temperature, then switched to NH$_3$ flow (30 ml/min) for 1 h. Finally, ramped to 700 °C at a heating rate of 10 °C/min under He flow. FT-IR of adsorbed pyridine was used to determine the nature of surface acid sites type.

Activity Tests and Product Analysis

The catalytic activity experiments was carried out in a round bottom flask, to which was added 3 ml (DMSO), 50 mg of glucose and 20 mg of catalyst. Then, it was heated desired reaction temperature in an oil-bath with a magnetic stirrer. After specified time, the round bottom flask was removed from the oil bath and cooled to room temperature. Then, the reaction mass was centrifuged to separate the catalyst, and the HMF yield was analyzed by HPLC using a C-18 column (250 mm × 4.6 mm) and equipped with UV-detector. A mixture of 4:6 (v:v) acetonitrile:water was used as the mobile phase at a flow rate of 0.5 ml/min. The glucose conversion was determined by HPLC fitted with HPX-87H column (Bio-Rad, Richmond, CA) and a refractive index (RI) detector. The glucose conversion, the yield of HMF and the selectivity of HMF were calculated according to the following formula.

Fig. 1 XRD patterns of ZA and BZA catalysts (*a*) ZA, (*b*) BZA-0.05, (*c*) BZA-0.10, (*d*) BZA-0.15, (*e*) BZA-0.20, (*f*) BZA-0.30

$$\text{Glucose conversion (mol\%)} = \left(1 - \frac{\text{Moles of glucose in products}}{\text{Starting moles of glucose}}\right) \times 100\% \tag{1}$$

$$\text{HMF yield (mol\%)} = \frac{\text{Moles of HMF in products}}{\text{Starting moles of glucose}} \times 100\% \tag{2}$$

$$\text{HMF selectivity (mol\%)} = \frac{\text{Moles of HMF in products}}{\text{Moles of reacted glucose}} \times 100\% \tag{3}$$

Results and Discussion

Characterization of Catalysts

The X-ray diffraction patterns of the ZA and BZA catalysts are presented in Fig. 1. The diffraction pattern of ZA sample revealed that monoclinic (m-ZrO_2) and tetragonal (t-ZrO_2) phases co-exist (Fig. 1a). The diffraction peaks at 2θ of 28.2° and 31.5° corresponding to the m-ZrO_2 phase. While the peaks at 2θ = 30.25°, 35.5°, 50.3° and 60° can be ascribed to the t-ZrO_2 phase. It is generally acknowledged that the tetragonal phase was more essential for formation of acidic centers [26]. Besides, no diffraction peaks related to the co-precipitated alumina oxide were found. This indicated that alumina oxide was dispersed on the support. However, addition of B_2O_3 caused drastic changes in the crystalline structure of ZrO_2. The m-ZrO_2 phase disappear and only the tetragonal phase of ZrO_2 exist (Fig. 1b–f). It is well known that a tetragonal phase of ZrO_2 starts to transform to monoclinic phase at >673 k due to loss of OH^- ions [27]. It may be that the B_2O_3
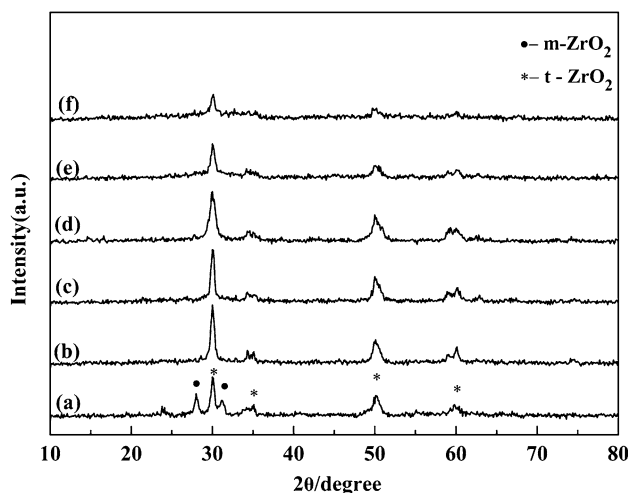
species stabilizes the tetragonal ZrO_2 phase. In addition, it is noteworthy that no diffraction line for the crystalline B_2O_3 phase was observed in the XRD patterns of BZA samples, suggesting that the supported B_2O_3 species were either amorphous state or highly dispersed with crystallite dimensions on the surface of ZA. The distributions of boron species of BZA-0.20 was measured by EDX using STEM mode. The TEM image results revealed that BZA-0.20 catalyst was amorphous (Fig. 2a). And amorphous boron species homogeneous distributions in the sample (Fig. 2b). Additionally, Al, Zr and O were also observed with homogeneous distributions, as illustrated in Fig. 2c–e, which is good agreement with the XRD analysis.

Figure 3 displays the FT-IR spectra of ZA and BZA catalysts. The bands at 3435 and 1636 cm⁻¹ can be assigned to the O–H stretching vibration of the physically absorbed water molecules and the HOH bending vibration of H_2O. The band located around 501 cm⁻¹ can be ascribed to the Zr–O vibration. The IR spectra of BZA samples commonly exhibited the new peaks around at 1050–1150 and 885 cm⁻¹ were attributed to BO_4 asymmetric stretches and BO_3 symmetric stretching, respectively. The newly band at 1400–1450 cm⁻¹ belonged to BO_3 asymmetric stretches. Along with increasing the loading of B_2O_3, the intensity of this band was detected to increase with a gradual shift to a higher wavenumber from 1400 to 1450 cm⁻¹ (Fig. 3b–f), which suggested an increasing formation of BO_3 units at higher loading of B_2O_3. By comparison with the spectra of boric acid (only trigonal BO_3 units) and borax (both
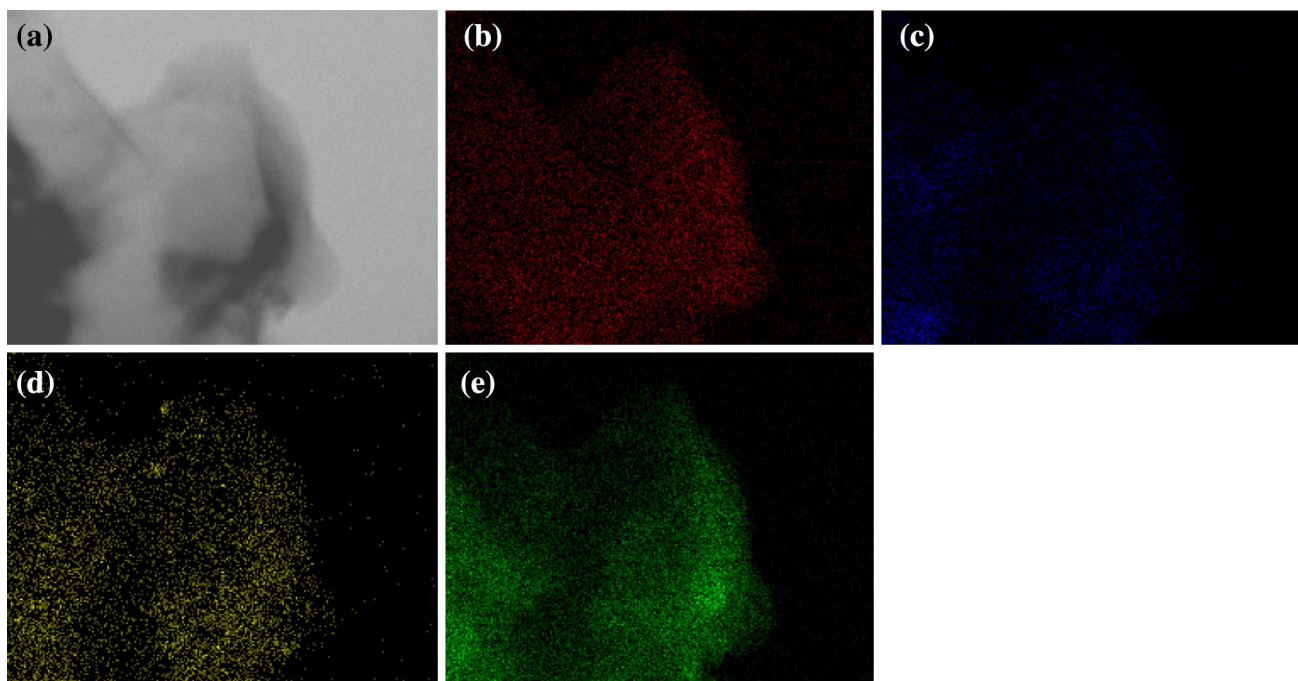
Fig. 2 TEM images **a** and elemental maps of BZA-0.20 (**b–f**) **b** the EDX map of B, **c** the map of Al, **d** the map of Zr, **e** the map of O
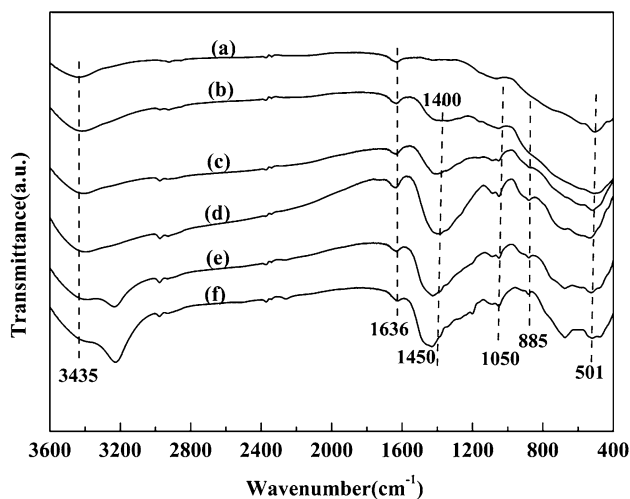

Fig. 3 FT-IR spectrum of ZA and BZA catalysts (*a*) ZA, (*b*) BZA-0.05, (*c*) BZA-0.10, (*d*) BZA-0.15, (*e*) BZA-0.20, (*f*) BZA-0.30

trigonal BO_3 and tetrahedral BO_4 units) (Fig. 1s), the bands at 1400–1460, 885 cm^{-1} represent formation of BO_3 units, while the band at 1050–1150 cm^{-1} represent formation of BO_4 units [28]. The above result indicated that both trigonal and tetrahedral boron species exist on the surface of BZA samples.

Figure 4 shows the X-ray photoelectron spectroscopy (XPS) measurements results of BZA-0.20. The B1s, Al2p, Zr3d, O1s peaks of the sample in Fig. 4a were consistent

with the main element compositions of BZA-0.20. Moreover, B was obviously found in the sample, which reflected that boron species existed in the catalyst. The binding energy at 192.9 eV (Fig. 4b) is related to the B–O–B bonds in B_2O_3 or H_3BO_3 [29]. Figure 4c displays the binding energy of the Al2p photoelectron peak at around 74.3 eV. The Zr spectrum (Fig. 4d) showed two peaks at 182.2 and 184.9 eV correspond to the $Zr3d_{5/2}$ and $Zr3d_{3/2}$ spin-orbitals of Zr^{4+}, respectively. Normally, the $Zr3d_{3/2}$ line in the case of pure ZrO_2 samples can be seen at 184.5 eV. A slight increase in this study may be due to the incorporation of Al_2O_3 in the sample. The photoelectron peaks at 531.5 eV is assigned to the binding energy of O1s. The results further illustrated the successfully introduction of B_2O_3 in the surface of ZA.

The acid strength and density of BZA-0.20 were determined by NH_3-TPD measurement. The acid sites could be measured as weak, medium, strong and super-strong at desorption temperatures of 100–250, 250–350, 350–500, and >500 °C, respectively [30]. As shown in Fig. 2s, it can be detected that the catalyst possesses two main desorption peaks: one large peak at a temperature of around 130 °C related to weak acid sites: a small NH_3 desorption peak around at 360 °C classified as strong acid sites center. The results deduced that introduction of boron species in the structure of ZA is mainly formed the weak acid sites center. As illustrated in Table 1, the total amount of acidic increased initially and then decreased when B_2O_3 loading was increased. The total amount of acidic sites of
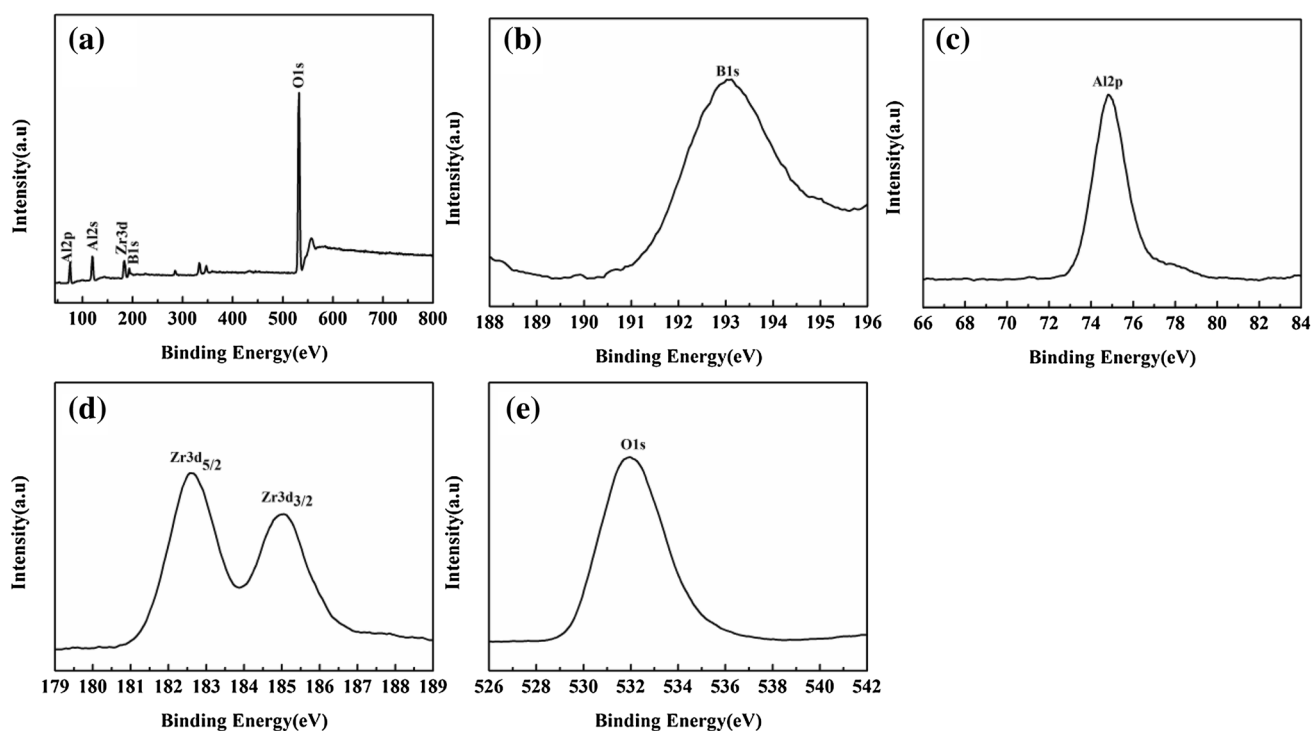
Fig. 4 The XPS spectrum of BZA-0.20. **a** Survey scan, **b** B1s spectrum, **c** Al2p spectrum, **d** Zr3d spectrum, **e** O1s spectrum

Table 1 Physicochemical properties of BZA catalysts

Entry	Sample	Surface area (m^2/g)	Total acid density $(\mu mol/g)^a$
1	ZA	36.6	136
2	BZA-0.05	46.5	279
3	BZA-0.10	53.8	288
4	BZA-0.15	57.5	362
5	BZA-0.20	105.0	436
6	BZA-0.30	81.1	290

[a]Total acid density quantified by NH_3-TPD

Fig. 5 The pyridine adsorption IR spectra of BZA-0.20

BZA-0.20 is highest, attaining 436 μmol/g. The decrease in the acidity observed for BZA-0.30 (290 μmol/g) may be because of a slight decrease in the surface area.

Meanwhile, Table 1 also illustrated the BET surface area results of all the catalysts. The BET surface area gradually increases with the increase of B_2O_3 loading and reaches a maximum for BZA-0.20 (20 wt%, $S_{BET} = 105.0$ m^2/g). However, further increasing B_2O_3 loading to 30 wt% will lead to BET surface area decrease (BZA-0.30, $S_{BET} = 81.1$ m^2/g), which is consistent with the previous literature [24, 31, 32].

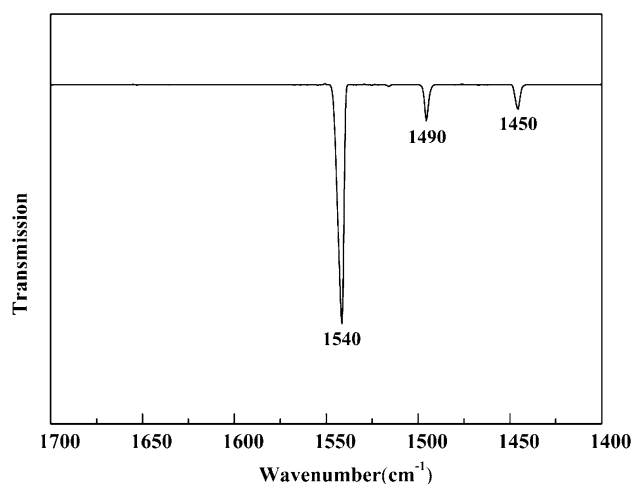Furthermore, in order to determine the nature of acid sites in the BZA samples, Pyridine FT-IR spectra was given in Fig. 5. The band at around 1450 cm^{-1} is associated to the characteristic of pyridine adsorbed on weak Lewis acid sites. The band at 1540 cm^{-1} is also detected, correlated to the stretching vibrations of C–N of pyridine with Brønsted acid sites. While the band at 1490 cm^{-1} corresponded to the characteristic of pyridine adsorbed to Lewis acid and Brønsted acid sites. These findings suggest that the BZA catalysts possesses Lewis acid and Brønsted acid sites.

Table 2 Effects of various catalysts on dehydration of glucose to HMF

Entry	Sample	Conversion (%)	HMF yield (%)
1	Without catalyst	74.5	10.5
2	ZrO_2	76.6	12.3
3	ZA	80.7	18.9
4	H_3BO_3	87.7	24.8
5	$B_2O_3(20\ wt\%)/ZrO_2$	83.6	21.1
6	$B_2O_3(20\ wt\%)/Al_2O_3$	89.1	31.8
7	BZA-0.20	90.8	41.2

Reaction conditions: 50 mg of glucose, 20 mg of catalyst, 3 ml of DMSO, 4 h, 150 °C

Synthesis of HMF from Glucose Catalyzed by Various Catalysts

Table 2 showed the results that the influence of various catalysts on transformation of glucose to HMF in DMSO solvent. The ZrO_2, ZA, H_3BO_3, $B_2O_3(20\ wt\%)/ZrO_2$, $B_2O_3(20\ wt\%)/Al_2O_3$ and BZA-0.20 were used to catalyze glucose conversion. A low HMF yield of 10.5 and 74.5% glucose conversion was observed without a catalyst. The unfunctionalized metal oxide supports also showed poor catalytic performance, which could be ascribed to lack of Brønsted acid sites. Notably, $B_2O_3(20\ wt\%)/ZrO_2$ and $B_2O_3(20\ wt\%)/Al_2O_3$ afforded a moderate HMF yield of 21.1, 31.8% and glucose conversion (i.e., 83.6 and 89.1%, respectively) under identical reaction conditions. Among these catalysts, the BZA-0.20 catalyst showed the best catalytic performance for the conversion of glucose. This may be because the stable structure of BZA-0.20 at high temperature and the introduction of B_2O_3 improve the efficiency of the dehydration of glucose into HMF by combining the Lewis with Brønsted acid sites.

The BZA-0.20 catalysts is better than the most catalysts reported in the literature [13, 14, 17, 33], such as SO_4^{2-}/ZrO_2, SO_4^{2-}/SnO_2, SO_4^{2-}/Al_2O_3-SnO_2, mesoporous tantalum and mezsoporous aluminium doped MCM-41 silica. Jiménez-Morales used the mesoporousaluminium doped MCM-41 silica as catalyst conversion of glucose to HMF ; the best yield of HMF 36% at glucose conversion of 87% were achieved at 195 °C [33].

Effect of B_2O_3 Loading on the Dehydration of Glucose

The catalytic activity of BZA with different B_2O_3 loading was investigated, and the results are shown in Fig. 6. It is obviously that B_2O_3 loading accelerate the glucose dehydration process. The HMF yields of 24.1, 30.1, 35.5, 41.2 and 33.6% at glucose conversion of 82.6, 89.2, 90.1, 90.8 and 91.2% were obtained for BZA-0.05, BZA-0.10,
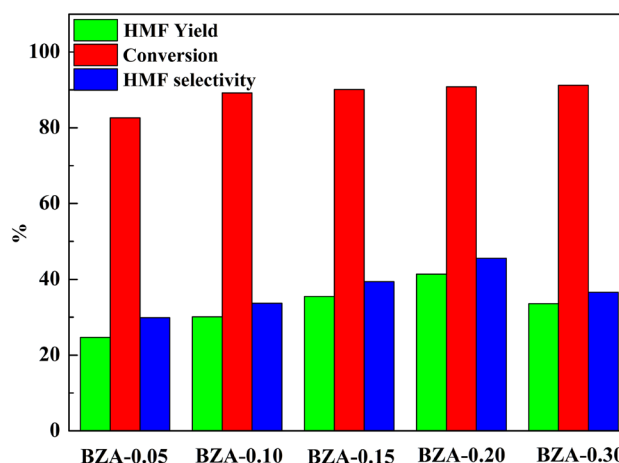

Fig. 6 Effect of the B_2O_3 loading on the dehydration of glucose. Reaction conditions: 50 mg of glucose, 20 mg of catalyst, 3 ml of DMSO, 4 h, 150 °C

BZA-0.15, BZA-0.20 and BZA-0.30. Among these BZA catalysts, BZA-0.20 showed best catalytic performance towards dehydration of glucose to HMF, which could be associated with its higher specific surface areas and total acid density. HMF yield decreased to 33.6% when the B_2O_3 loading was further increased to 30 wt% although a high glucose conversion of 91.2% was attained.These results confirm that there is a highly linear relationship between the yield of HMF and the total surface acidic amount. However, it is evidently that the HMF selectivity showed a different tendency. When the B_2O_3 loading increased from 5 to 20 wt%, the selectivity of HMF gradually increased from 29.9 to 45.6%. Further increment of B_2O_3 loading did not offer additional HMF selectivity. It might be related to the decrease of Lewis acid sites of sample BZA-0.30. Many reports have been proved that the glucose isomerization of glucose to HMF at the Lewis acid sites, then the Brønsted acid sites facilitate the fructose dehydration to HMF [15, 34, 35].

Effect of Reaction Temperature

In the following section, the influence of the different of temperatures on dehydration of glucose with BZA-0.20 was examined. The results are presented in Fig. 7. The glucose conversion is sensitive to reaction temperature. Glucose conversion increased from 76.2 to 92.4% with an increase the temperature from 130 to 170 °C. Up to 150 °C, the maximum HMF yield is achieved. While the temperature was further increased, did not enhance the reaction efficiency and even caused a loss of HMF yield. It was also observed that the selectivity of HMF gradually increased from 34.5% at 130 °C to 45.6% at 150 °C and then quickly decreased after 150 °C, this could be attributed to the
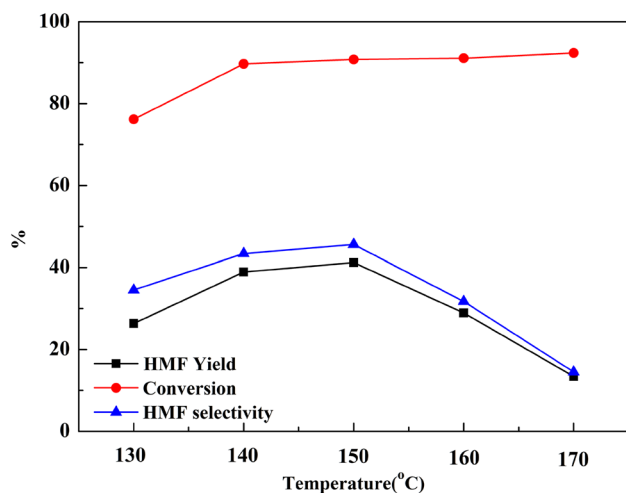
Fig. 7 Effect of the reaction temperatures. Reaction conditions: 50 mg of glucose, 20 mg of BZA-0.20, 3 ml of DMSO, 4 h

higher temperature promotes the HMF rehydrated into undesired by-products such as LA and formic acid, which in turn decreases the selectivity of HMF [36]. Thus, 150 °C was chosen as the optimal temperature for this reaction.

Effect of Reaction Time

Figure 8 shows the effect of reaction time on glucose conversion to HMF. With an increase of reaction time from 1 to 5 h, the glucose conversion increased readily. It is clear that the HMF yield and selectivity didn't follow this trend. In the range from 1 to 4 h, the HMF yield (21.7–41.2%) and selectivity (25.6–45.6%) exhibited significant increases. Whereas what happened next were that the yield and selectivity dropped to 30.1 and 32.7% at 5 h. These results
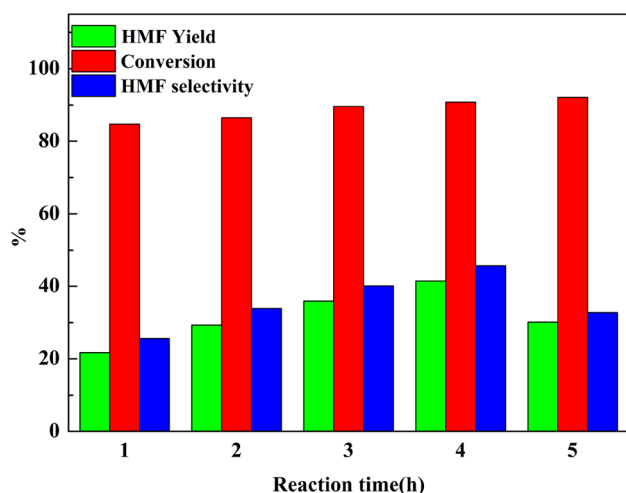
indicated that the formation of polymers species hinder the active sites with prolonging the reaction time, which could be confirmed through a change in the color of reaction mixture from brown to black [37]. Therefore, the reaction time of 4 h was selected as the optimum condition for glucose dehydration to HMF.

Effect of Catalyst Dosage

The influence of the catalyst dosage (i.e., 5, 10, 20, 30, 40 and 50 mg) on dehydration of glucose to HMF was tested at 150 °C for 4 h, the date was summarized in Fig. 9. It is notable to see that HMF yield correlated positively with BTA-0.20 dosage. The yield of HMF increased notably with the dosage increased from 5 to 20 mg. When the dosage of the catalyst was 20 mg showed excellent catalytic performance can be observed. With further increasing the catalyst dosage to 50 mg resulted in a decrease in the yield of HMF (i.e., 30.4%), besides the reaction solution gradually converted to a darker color, which indicates the formation of more humins. A similar trend was observed for the HMF selectivity. For example, HMF selectivity was 38.1% at 30 mg and 33.6% at 50 mg. It is possibly due to an excess amount of catalyst with superfluous acid sites would facilitate the interactions between the synthesis of HMF and the glucose on the catalyst surface, which lead to a lower HMF selectivity. Thus, it is meant that the reaction is less efficient with high amount of catalyst, since the additional substrate is preferential formation of by-products, such as polymers, humins and other compound [38]. Therefore, 20 mg BZA-0.20 dosage has been chosen for the dehydration of glucose to HMF in this work. Based on the above results of the reaction, the possible reaction pathway for glucose conversion to HMF was given in Scheme 1.
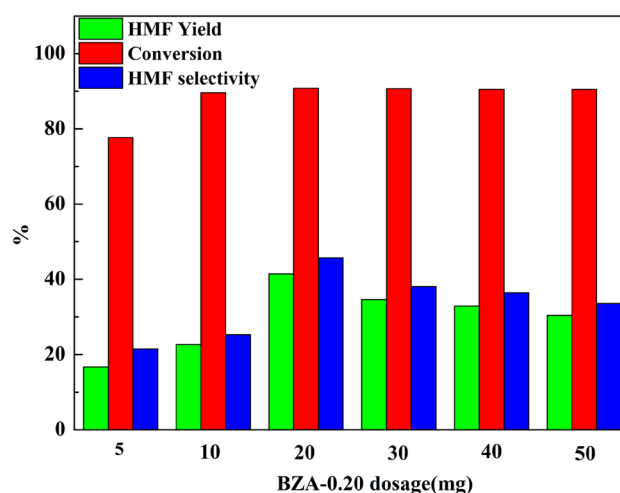

Fig. 8 Effect of the reaction time. Reaction conditions: 50 mg of glucose, 20 mg of BZA-0.20, 3 ml of DMSO, 150 °C

Fig. 9 Effect of the catalyst dosage. Reaction conditions: 50 mg of glucose, 3 ml of DMSO, 4 h, 150 °C

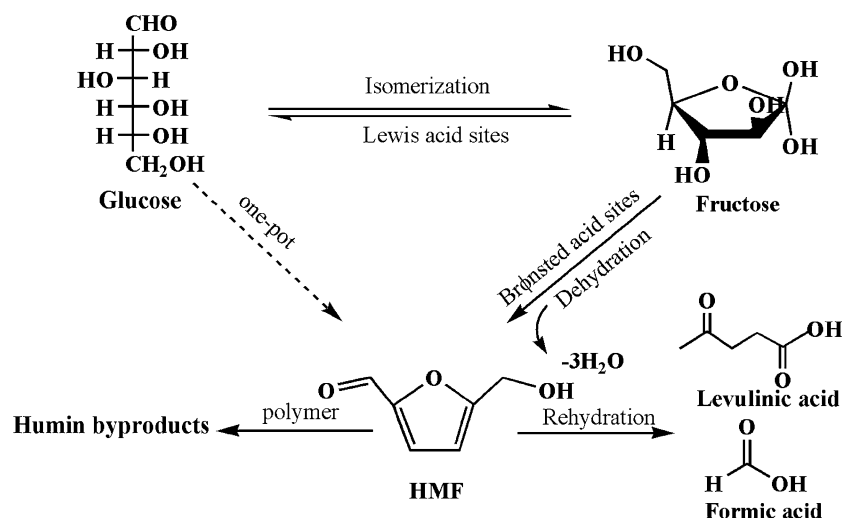**Scheme 1** The possible reaction pathway for glucose conversion to HMF

Table 3 Effect of different solvents for the conversion of glucose to HMF

Entry	Solvent	Conversion (%)	HMF yield (%)
1	DMSO	90.8	41.2
2	NMP	85.1	24.5
3	DMAC	81.6	19.1
4	DMF	79.7	17.2
5	[BMIM]Cl	90.5	29.2
6	DMSO+[BMIM]Cl[a]	81.0	25.9

Reaction conditions: 50 mg glucose, 20 mg of BZA-0.20, 3 ml DMSO, 150 °C, 4 h

[a]Volume ratio of DMSO/[BMIM]Cl = 5:1

Table 4 Dehydration of different substrates to HMF

Entry	Substrate	Time (h)	Temperature (°C)	HMF yield (%)
1	Fructose	2	120	61.9
2	Fructose	3	120	71.1
3	Maltose	4	150	35.7
4	Sucrose	2	150	50.8
5	Sucrose	3	150	64.6
6	Cellobiose	4	150	27.6
7	Cellulose	5	150	4.67
8	Starch	5	150	23.5

Reaction conditions: 50 mg of substrate, 3 ml of DMSO, 20 mg of BZA-0.20

Effect of Different Solvents for the Conversion of Glucose to HMF

The effect of the solvent on the dehydration of glucose to HMF is also investigated using different of solvents, including NMP, DMF, DMAC and [BMIM]Cl. The results are listed in Table 3. Among above the solvent, DMSO shows the best yield and conversion of glucose in this study. However, the other solvents, NMP, DMAC, DMF and [BMIM]Cl with moderate yields of HMF 24.5, 19.1, 17.2, 29.2% at glucose conversion 85.1, 81.6, 79.7, 90.5%, respectively. The key factor is that the side reactions were suppressed by DMSO, thus HMF could stable in the process of reaction [39, 40]. In addition, the high boiling point of the DMSO is also play a crucial role in the reaction. At the same time, we also examined the influence of co-solvent in the conversion of glucose to HMF. In the co-solvent DMSO/[BMIM]Cl system, only 25.9% yield of HMF was attained.

Effect of Different Biomass Materials on HMF Production

To further explore the applicability of the catalyst, the reaction was carried out with other carbohydrates, such as fructose, sucrose, maltose, cellobiose, cellulose and starch. The experimental results are summarized in Table 4. A high yield of HMF (71.1%) was obtained from fructose at 120 °C for 3 h. To our delight, a HMF yield of 64.6% was attained using sucrose as a starting feedstock. For the maltose and cellobiose the HMF yield of 35.7, 27.6% were achieved. Unfortunately, HMF yields with cellulose and starch were lower than those of glucose under same reaction conditions. The main reason is that the hydrolysis of these macromolecules to glucose is difficult in DMSO.

Reusability of the BZA-0.20

The stability of heterogeneous catalysts is of great importance in catalytic process. BZA-0.20 catalyst was separated by centrifugation from the mixture solvent after reaction,
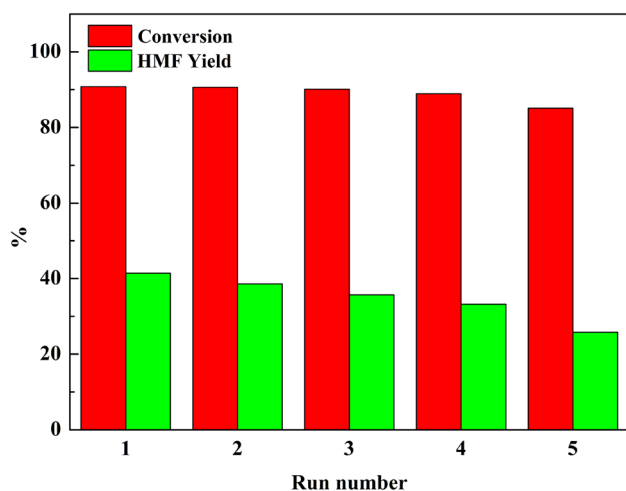
Fig. 10 Reusability of the BZA-0.20. Reaction conditions: 50 mg of glucose, 20 mg of BZA-0.20, 3 ml of DMSO, 4 h, 150 °C

washed with deionized water, ethanol and acetone, and dried at 80 °C, finally the recovered catalyst was calcined at 773 K for 1 h. The recyclability was conducted under optimized conditions (i.e., 50 mg glucose, 20 mg BZA-0.20, 3 ml DMSO, 150 °C and 4 h). As shown in Fig. 10, the yield of fresh BZA-0.20 is about 41.2%. After the first two experiments, no obvious loss of HMF was observed, but the catalytic activity of the BZA-0.20 showed a significant decrease after the fifth run. This demonstrated that the catalyst of BZA can be reused, but the recycling time is limited. The FTIR spectrum (Fig. 3s) and XRD pattern (Fig. 4s) of the recovered BZA-0.20 are well consistent with those of the fresh one. On the other hand, the surface area and total acid density of the recovered BZA-0.20 decreased to 64.3 m^2/g and 281 µmol/g, as compared with that of fresh one (105 m^2/g and 436 µmol/g).

Conclusion

In summary, a series of BZA solid acid catalysts with Lewis and Brønsted acid sites were successfully synthesized and carried out for production of HMF from glucose in DMSO solvent under mild conditions. The catalyst BZA-0.20 exhibited superior activity and a HMF yield of 41.2% at the glucose conversion of 90.8% was obtained at 150 °C for 4 h. The catalytic system also displayed a good catalytic activity for transformation biomass-derived carbohydrates to HMF. These results could be related to the surface area (105 m^2/g), and suitable acidity (436 µmol/g) of BZA-0.20. Besides, the presence of both Lewis and Brønsted acid sites promote the isomerization of glucose to fructose and fructose dehydration to HMF in this reaction.

References

1. Ragauskas, A.J., Williams, C.K., Davison, B.H.: The path forward for biofuels and biomaterials. Science **311**, 484–489 (2006)
2. Liu, B., Zhang, Z.: Catalytic conversion of biomass into chemicals and fuels over magnetic catalysts. ACS Catal. **6**, 326–338 (2016)
3. Pan, J., Gao, H.P., Zhang, Y.L., et al: Porous solid acid with high surface area derived from emulsion templating and hyper-crosslinking for efficient one-pot conversion of cellulose to 5-hydroxymethylfurfural. RSC Adv. **4**, 59175–59184 (2014)
4. Zhang, Z., Deng, K.: Recent advances in the catalytic synthesis of 2, 5-furandicarboxylic acid and its derivatives. ACS Catal. **5**, 6529–6544 (2015)
5. Zhou, P., Zhang, Z.: One-pot catalytic conversion of carbohydrates into furfural and 5-hydroxymethylfurfural. Catal. Sci. Technol. **6**, 3694–3712 (2016)
6. Liu, B., Zhang, Z.: One-pot conversion of carbohydrates into furan derivatives via furfural and 5-hydroxylmethylfurfural as intermediates. ChemSusChem. **9**, 2015–2036 (2016)
7. Rosatella, A.A., Simeonov, S.P., Frade, R.F.M., et al.: 5-Hydroxymethylfurfural (HMF) as a building block platform: Biological properties, synthesis and synthetic applications. Green Chem. **13**, 754–793 (2011)
8. Chheda, J.N., Román-Leshkov, Y., Dumesic, J.A.: Production of 5-hydroxymethylfurfural and furfural by dehydration of biomass-derived mono-and poly-saccharides. Green Chem. **9**, 342–350 (2007)
9. Atanda, L., Silahua, A., Mukundan, S., et al.: Catalytic behaviour of TiO$_2$-ZrO$_2$ binary oxide synthesized by sol–gel process for glucose conversion to 5-hydroxymethylfurfural. RSC Adv. **5**, 80346–80352 (2015)
10. Wang, T., Nolte, M.W., Shanks, B.H.: Catalytic dehydration of C6 carbohydrates for the production of hydroxymethylfurfural (HMF) as a versatile platform chemical. Green Chem. **16**, 548–572 (2014)
11. Girka, Q., Estrine, B., Hoffmann, N., et al.: Simple efficient one-pot synthesis of 5-hydroxymethylfurfural and 2, 5-diformylfuran from carbohydrates. React. Chem. Eng. **1**, 176–182 (2016)
12. Zhao, H., Holladay, J.E., Brown, H., Zhang, Z.C.: Metal chloridesin ionic liquid solvents convert sugars to 5-hydroxymethylfurfural. Science **316**, 1597–1600 (2007)
13. Osatiashtiani, A., Lee, A.F., Brown, D.R., et al.: Bifunctional SO$_4^{2-}$/ZrO$_2$ catalysts for 5-hydroxymethylfufural (5-HMF) production from glucose. Catal. Sci. Technol. **4**, 333–342 (2014)
14. Lopes, M., Dussan, K., Leahy, J.J., et al.: Conversion of D-glucose to 5-hydroxymethylfurfural using Al$_2$O$_3$-promoted sulphated tin oxide as catalyst. Catal. Today **279**, 233–243 (2017)
15. Xu, S., Yan, X., Bu, Q., et al.: Highly efficient conversion of carbohydrates into 5-hydroxymethylfurfural using the bi-functional CrPO$_4$ catalyst. RSC Adv. **6**, 8048–8052 (2016)
16. Chen, D., Liang, F., Feng, D., et al.: An efficient route from reproducible glucose to 5-hydroxymethylfurfural catalyzed by porous coordination polymer heterogeneous catalysts. Chem. Eng. J. **300**, 177–184 (2016)
17. Jiménez-Morales, I., Moreno-Recio, M., Santamaría-González, J., et al.: Mesoporous tantalum oxide as catalyst for dehydration of glucose to 5-hydroxymethylfurfural. Appl. Catal. B **154**, 190–196 (2014)

18. Wang, Y., Tong, X., Yan, Y., et al.: Efficient and selective conversion of hexose to 5-hydroxymethylfurfural with tin–zirconium-containing heterogeneous catalysts. Catal. Commun. **50**, 38–43 (2014)

19. Mendicino, J.F.: Effect of borate on the alkali-catalyzed isomerization of sugars1. J. Am. Chem. Soc. **82**(18), 4975–4979 (1960)

20. Gao, H.P., Peng Y.X., Pan, J.M, et al.: Synthesis and evaluation of macroporous polymerized solid acid derived from pickering HIPEs for catalyzing cellulose into 5-hydroxymethylfurfural in an ionic liquid. RSC Adv. **4**(81), 43029–43038 (2014)

21. Hansen, T.S., Mielby, J., Riisager, A.: Synergy of boric acid and added salts in the catalytic dehydration of hexoses to 5-hydroxymethylfurfural in water. Green Chem. **13**, 109–114 (2011)

22. Walia, M., Sharma, U., Agnihotri, V.K., et al.: Silica-supported boric acid assisted conversion of mono-and poly-saccharides to 5-hydroxymethylfurfural in ionic liquid. RSC Adv. **4**, 14414–14418 (2014)

23. Khokhlova, E.A., Kachala, V.V., Ananikov, V.P.: The first molecular level monitoring of carbohydrate conversion to 5-hydroxymethylfurfural in Ionic Liquids. B_2O_3-an efficient dual-function metal-free promoter for environmentally benign applications. ChemSusChem. **5**, 783–789 (2012)

24. Liu, J., Li, H., Liu, Y.C., et al.: Catalytic conversion of glucose to 5-hydroxymethylfurfural over nano-sized mesoporous Al_2O_3-B_2O_3 solid acids. Catal. Commun. **62**, 19–23 (2015)

25. Osiglio, L., Romanelli, G., Blanco, M.: Alcohol acetylation with acetic acid using borated zirconia as catalyst. J. Mol. Catal. A **316**, 52–58 (2010)

26. Sun, W., Zhao, Z., Guo, C., et al.: Study of the alkylation of isobutane with n-butene over WO_3/ZrO_2 strong solid acid. 1. Effect of the preparation method, WO_3 loading, and calcination temperature. Ind. Eng. Chem. Res. **39**, 3717–3725 (2000).

27. Gomez, R., Lopez, T., Bokhimi, X., et al.: Dehydroxylation and the crystalline phases in sol-gel zirconia. J. Sol-gel Sci. Technol. **11**, 309–319 (1998)

28. Mao, D., Lu, G., Chen, Q.: Deactivation and regeneration of the B_2O_3/TiO_2-ZrO_2 catalyst in the vapor phase Beckmann rearrangement of cyclohexanone oxime. J. Mol. Catal. A **240**, 164–171 (2005)

29. Zhu, L.Y., Wang, X.Q., Zhang, G.H., et al.: Structural characterization and photocatalytic activity of B_2O_3/ZrO_2-TiO_2 mesoporous fibers. Appl. Catal. B **103**, 428–435 (2011)

30. Liu, D., Yuan, P., Liu, H., et al.: Quantitative characterization of the solid acidity of montmorillonite using combined FTIR and TPD based on the NH_3 adsorption system. Appl. Clay Sci. **80**, 407–412 (2013)

31. Jiao, H., Zhao, X., Lu, C., et al.: Nb_2O_5-γ-Al_2O_3 nanofibers as heterogeneous catalysts for efficient conversion of glucose to 5-hydroxymethylfurfural. Sci. Rep. **6**, (2016)

32. Sinhamahapatra, A., Pal, P., Tarafdar, A., et al.: Mesoporous borated zirconia: A solid acid-base bifunctional catalyst. ChemCatChem. **5**, 331–338 (2013)

33. Jiménez-Morales, I., Moreno-Recio, M., Santamaría-González, J., et al.: Production of 5-hydroxymethylfurfural from glucose using aluminium doped MCM-41 silica as acid catalyst. Appl. Catal. B **164**, 70–76 (2015)

34. Wang, X., Zhang, H., Ma, J., et al.: Bifunctional Brønsted–Lewis solid acid as a recyclable catalyst for conversion of glucose to 5-hydroxymethylfurfural and its hydrophobicity effect. RSC Adv. **6**, 43152–43158 (2016)

35. Moreno-Recio, M., Santamaría-González, J., Maireles-Torres, P.: Brönsted and Lewis acid ZSM-5 zeolites for the catalytic dehydration of glucose into 5-hydroxymethylfurfural. Chem. Eng. J. **303**, 22–30 (2016)

36. Huang, R., Qi, W., Su, R., et al.: Integrating enzymatic and acid catalysis to convert glucose into 5-hydroxymethylfurfural. Chem. Commun. **46**, 1115–1117 (2010)

37. Cai, H., Li, C., Wang, A., et al.: Zeolite-promoted hydrolysis of cellulose in ionic liquid, insight into the mutual behavior of zeolite, cellulose and ionic liquid. Appl. Catal. B **123**, 333–338 (2012)

38. Román-Leshkov, Y., Moliner, M., Labinger, J.A., et al: Mechanism of glucose isomerization using a solid Lewis acid catalyst in water. Angew. Chem. Int. Ed. **49**, 8954–8957 (2010)

39. Hicks, K.B., Symanski, E.V., Pfeffer, P.E.: Synthesis and high-performance liquid chromatography of maltulose and cellobiulose. Carbohydr. Res. **112**, 37–50 (1983)

40. Liu, W., Wang, Y., Li, W., et al.: Polyethylene glycol-400-functionalized dicationic acidic ionic liquids for highly efficient conversion of fructose into 5-hydroxymethylfurfural. Catal. Lett. **145**, 1080–1088 (2015)